Int. J. Electrochem. Sci., 12 **(2017)** 3197 – 3211, doi: 10.20964/2017.04.04

International Journal of
ELECTROCHEMICAL
SCIENCE
www.electrochemsci.org

Electrochemical Behavior of Gallium-Doped Lithium Titanate in a Wide Range of Potentials

Tatiana Kulova[1,*], *Anna Kuz'mina*[1], *Alexander Skundin*[1], *Irina Stenina*[2], *Andrei Yaroslavtsev*[2]

[1] Frumkin Institute of Physical Chemistry and Electrochemistry of the Russian Academy of Sciences, 31-4 Leninskii prospect, Moscow, 119071, Russia
[2] Kurnakov Institute of General and Inorganic Chemistry of the Russian Academy of Sciences, 31 Leninskii prospect, Moscow, 119991, Russia
[*]E-mail: tkulova@mail.ru

Received: 29 December 2016 / *Accepted:* 20 January 2017 / *Published:* 12 March 2017

A synthesis method of gallium-doped lithium titanate is proposed. The effect of gallium-doping on electrochemical properties of the $Li_{4+x-3y}Ti_{5-x}Ga_{x+y}O_{12}$ (x+y = 0.2; y/x=2.56) is studied in detail. It has been established that the cycling range extension leads to a reversible insertion of more than four lithium ions per formula unit of gallium-doped lithium titanate, which corresponds to a reversible capacity of about 280 mAh g^{-1}. Gallium doping results in the increased cycling stability of lithium titanate in a wide range of potentials. The good electrochemical performance of the gallium-doped lithium titanate can be attributed to the increase in conductivity and effective diffusion coefficient.

Keywords: Gallium doping, lithium titanate, wide potential range, lithium-ion battery

1. INTRODUCTION

Nowadays lithium titanate is regarded as a promising anode material for lithium-ion batteries. It is conditioned by its ability to operate at increased C-rates up to 20 C. Theoretical capacity at the insertion of three lithium ions per one formula unit of lithium titanate amounts to about 175 mAh g^{-1}, in this case the charge-discharge curve represents a plateau at the potentials of about 1.55 V, which is conditioned by the existence of two phases: delithiated ($Li_4Ti_5O_{12}$) and lithiated ($Li_7Ti_5O_{12}$) [1, 2].

$$Li_4Ti_5O_{12} + 3e^- + 3Li^+ = Li_7Ti_5O_{12} \quad (1)$$

Small change in the size of a cubic cell of this compound (from 8.3595 to 8.3538 Å [3]) determines high cycling stability of the material. The number of charge-discharge cycles can go up to several thousand without significant degradation [4].

Theoretically, at the recovery of the whole of titanium to the oxidation state +3, up to 5 lithium ions per formula unit can get inserted into lithium titanate, which corresponds to the theoretical capacity of about 290 mAh g^{-1}. However, this deep lithiation (to near-zero potential), as a rule, results in accelerated degradation [5, 6]. At the same time, the authors [5, 6] did not register any changes in the unit cell at deep lithiation.

Relatively low electronic and lithium conductivity (10^{-13} S cm^{-1}) [7-10], as well as low discharge capacity, which is less than that of graphite and substantially less than that of silicon or tin [2], can be qualified as disadvantages of $Li_4Ti_5O_{12}$. However, these disadvantages are largely compensated by high cycling stability, especially at high charge/discharge currents, while silicon and tin quickly lose their initial capacity due to degradation resulting from significant volume change at lithium intercalation.

In order to increase electronic and lithium conductivity, there were attempts of heterovalent doping of $Li_4Ti_5O_{12}$ with divalent (Cu^{2+}), trivalent (Cr^{3+}, Sc^{3+}, Al^{3+}, Tb^{3+}) and pentavalent (Ta^{5+}) cations [11-17]. In a number of cases, increased conductivity of obtained materials was observed but electrochemical properties of the doped $Li_4Ti_5O_{12}$ were not studied.

A number of authors have reported results of study of electrochemical performances of the doped lithium titanates, but the range of cycling was from 1 to 3 V [14, 15, 17-19].

In our previous paper, we shortly reported the results of synthesis and galvanostatic cycling of gallium-doped lithium titanate [20]. The objective of this work is to synthesize gallium-doped lithium titanate and study lithium insertion and extraction processes in a wide range of potentials (from 3 to 0.01 V) in detail. The novelty of this work consists in the synthesis of gallium-doped lithium titanate with using citrate method as well as in the comprehensive study of the electrochemical characteristics of the material in a wide potential range (0.01 to 3 V), including the determination of discharge capacity at different current densities, and the calculation of the lithium diffusion coefficient in the solid phase. Only one paper concerning study of gallium-doped lithium titanate behavior in a narrow potential range can be found [21], and this fact emphasizes the importance of the present work.

2. EXPERIMENTAL

2.1. Synthesis of gallium-doped lithium titanate

Gallium-doped lithium titanate was synthesized using the citrate method. Titanium tetrabutylate (99%, Alfa Aesar) and lithium carbonate (99%, Fluka) were dissolved in the ethanol-nitric acid mixture (volume ratio 5:1), and solutions of gallium (99.99%, Aldrich) in nitric acid and citric acid (98%, Sigma) were added in the minimum quantity of water. Lithium carbonate was taken with a 5% surplus to prevent possible losses of lithium during subsequent annealing at high temperatures. The obtained mixture was heated sequentially at 95°C for 24 hours and at 250°C for 5 hours. The so formed precursor was ground in an agate mortar to a smooth paste that was subjected to final annealing at 800°C for 5 hours in air.

2.2. Physical characterization and electrochemical measurements

The crystal structure of the synthesized product was characterized by X-ray diffraction (XRD) with the CuKα radiation performed on Rigaku D/MAX 2200 diffractometer. The Rigaku Application Data Processing software package was used for spectra processing.

The microstructure of obtained samples was analyzed with Carl Zeiss NVision 40 scanning election microscope.

The study of electrochemical properties of lithium titanate samples was conducted in three-electrode sealed electrochemical cells with a lithium auxiliary electrode and a lithium reference electrode. Working electrodes were prepared using a standard paste method. Stainless steel mesh was used as a current collector. The active mass was prepared by mixing the lithium titanate powder (80% wt), carbon black (15% wt, Timcal, Belgium) and polyvinylidenfluoride (5% wt, Aldrich) predissolved in N-methylpyrrolidone (Aldrich). The loading of active material in the electrode was about 8–10 mg cm^{-2}. Electrodes were pressed under a pressure of 1,000 kg cm^{-2} with subsequent vacuum drying at 120^{o}C. Electrochemical cells were assembled in an argon-filled glove box ("Spectro-systems", Russia). The 1 M $LiPF_6$ in a mixture of ethylene carbonate-diethyl carbonate-dimethyl carbonate (1:1:1) (all components of the electrolyte were qualified as 'extra dry' and were purchased from Aldrich) was used as an electrolyte. Water content in the electrolyte did not exceed 10 ppm. Polypropylene nonwoven film of 20 μm (NPO "Ufim") was used as a separator. Electrochemical cycling of the cells was performed over the potential window of 0.01–3.0 V using a ZRU 50 mA–10 V charge-discharge system (NTT Buster JSC, Russia). The tests were performed under the galvanostatic regime at a current density of 20, 100, 200, 400, 800, 1600 and 3200 mA g^{-1}. Cyclic voltammetry was performed using an Elins P-8NANO (TzVA) potentiostat (Chernogolovka, Russia); potential scanning rates were 0.1, 0.2, 0.4, 0.8 mV s^{-1} over the potential window ranging from 0.01 to 3.0 V. Specific capacity was calculated per unit weight of the lithium titanate.

3. RESULTS AND DISCUSSION

3.1. Characterization of gallium-doped lithium titanate

X-ray patterns of $Li_4Ti_5O_{12}$ samples contain reflexes of $Li_4Ti_5O_{12}$ only (Card No. 72-0426 PDF2 database), which evidences that the obtained material is single-phase. Initially, the formula of $Li_{4+z}Ti_{5-z}Ga_zO_{12}$, where z is the degree of doping, was proposed for gallium-doped lithium titanate. Additional weak lines inherent in Li_2TiO_3 can be detected in $Li_{4+z}Ti_{5-z}Ga_zO_{12}$ at z = 0.2 [20]. An additional point is that all X-ray patterns display a lines shift to the high-angle region, which evidences of a decreased lattice parameter. In fact, with the growth of the degree of doping, the *a* parameter decreases from 8.3596(6) for $Li_4Ti_5O_{12}$ to 8.3537(4) for $Li_{4+z}Ti_{5-z}Ga_zO_{12}$.

It can be conditioned by the fact that radii of cations of Ga^{3+}, Ti^{4+} and Li^{+} are close, that is why gallium ions can get inserted into both, positions of titanium, and positions of lithium. Ga^{3+} ion attracts oxygen ions more intensively than Li^{+} ion considering Coulomb interaction, which results in a grater

lattice contraction. To verify this assumption, the structure of the doped sample was updated using the Rietveld method. Since the sample of doped lithium titanate with the degree of doping 0.2 contains small quantity of impurities (Li_2TiO_3), and the degree of doping is rather low, the structure was updated for the material of $Li_{4+z}Ti_{5-z}Ga_zO_{12}$ composition at z=0.1. The same tendency in the distribution of gallium was supposed to be preserved for the degree of gallium doping z=0.2. According to the data obtained as a result of updating the structure using the Rietveld method of the sample of $Li_{4+z}Ti_{5-z}Ga_zO_{12}$ composition at z=0.1 (Tables 1, 2), gallium ions occupy both, positions of lithium (8a), and positions of titanium (16d). Moreover, there are about 2.5 times less of gallium ions in octahedral sites than in tetrahedral ones. In accordance with these results, the formula of gallium-doped lithium titanate should be as follows: $Li_{4+x-3y}Ti_{5-x}Ga_{x+y}O_{12}$ (x+y=0.1-0.2; y/x=2.56). The obtained data agree with the observed dependence of lattice parameters on the doping level. Thus, when the doping degree are x+y=0.1 or x+y=0.2, the formulas are as follows: $Li_{3.812}Ti_{4.972}Ga_{0.1}O_{12}$ and $Li_{3.624}Ti_{4.944}Ga_{0.2}O_{12}$.

Table 1. Results of updating the structure of $Li_{3.812}Ti_{4.972}Ga_{0.1}O_{12}$ at 25°C.

Lattice type	Cubic lattice
Space group, Z	*Fd-3m*, 8
Scan space, 2Θ°	10-100
Scanning pitch	0.02
Lattice parameters, nm	*a* = 0.83544(1)
Cell volume, Å^3	583.102(16)
Number of reflexes	24
Bragg R-factor, Rf-factor	0.0489,0.0533
Rp, Rwp	0.0895, 0.133

Table 2. Coordinates of atoms and isotropic parameters of thermal bias (B) at 25°C

Atom	Symmetry of the site	Population	x	y	z	Biso
Li1	8a	0.976	0.1250	0.1250	0.1250	0.25(2)
Ga1	8a	0.024	0.1250	0.1250	0.1250	0.25(2)
Li2	16d	0.167	0.5000	0.5000	0.5000	0.46(3)
Ti	16d	0.828	0.5000	0.5000	0.5000	0.46(3)
Ga2	16d	0.005	0.5000	0.5000	0.5000	0.46(3)
O	32e	1.000	0.2618(2)	0.2618(2)	0.2618(2)	0.52(2)

According to the data from the scanning electron microscopy, synthesized samples of $Li_{3.812}Ti_{4.972}Ga_{0.1}O_{12}$ represent a rather homogeneous crystalline mass (Fig. 1a). Growth steps are clearly seen in the micrographs. At doping the size of particles slightly increases. The particle surface becomes smoother due to blurred facets. It is fair to assume that there is a partial melting of the sample. The size of particles for the undoped compound (x+y=0) varies within the range of 400-500 nm, for x+y=0.1 – 450-550 nm, for x+y=0.2 – 600-770 nm (Fig. 1b). Following the results of electron

probe microanalysis, there are cations of titanium, gallium and oxygen in all the studied areas of the sample. For doped titanate, the ratio of Ga/Ti is 0.2/5.2, which is almost the same as the initial load.

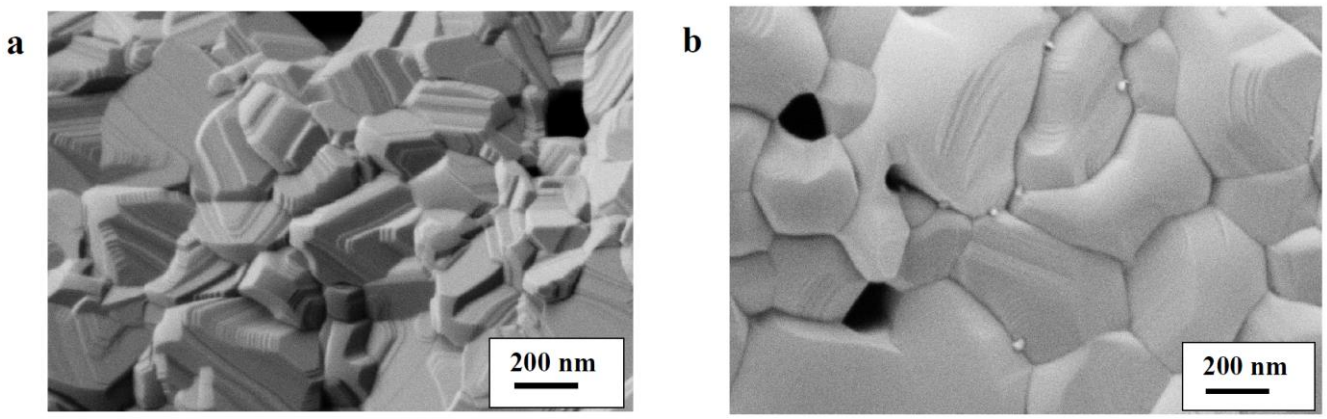

Figure 1. Scanning electron microscopy of the samples of $Li_{3.812}Ti_{4.972}Ga_{0.1}O_{12}$ (a) and $Li_{3.624}Ti_{4.944}Ga_{0.2}O_{12}$ (b).

3.2 Electrochemical insertion and extraction of lithium in $Li_{3.624}Ti_{4.944}Ga_{0.2}O_{12}$ and $Li_4Ti_5O_{12}$

During the study of lithium titanate in a three-electrode electrochemical cell with a lithium metal counter electrode, the cathode process of lithium insertion corresponds to charging of lithium titanate, and the anode process of lithium extraction – to discharging of lithium titanate in lithium-ion batteries. At the first stage, lithium insertion and extraction processes in the standard range of potentials (3 – 1 V) were studied.

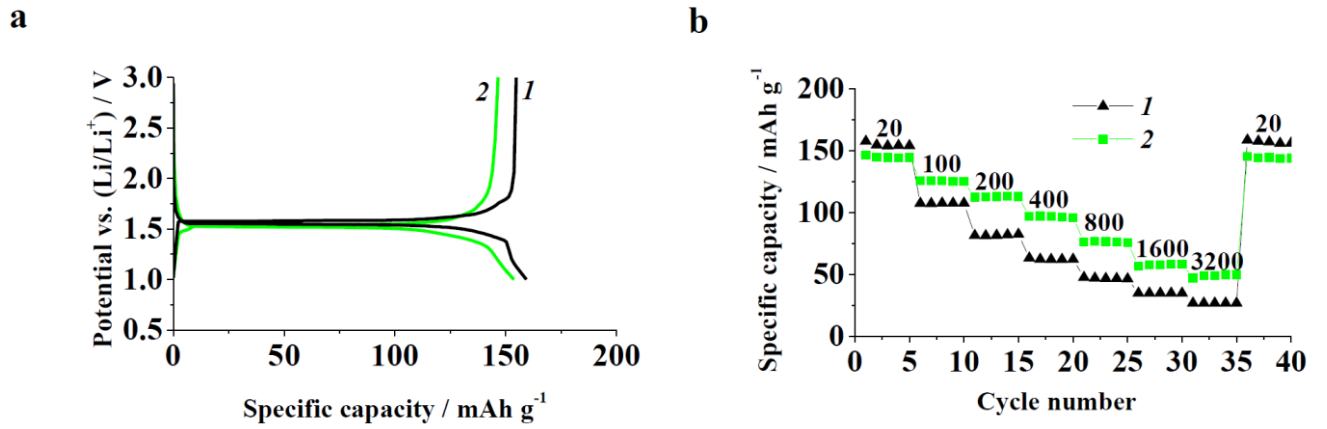

Figure 2. (a) Charge-discharge curves at the current density of 20 mA g^{-1} and (b) dependence of the discharge capacity on the current density (see values in the Figure) at the cycling in the range of potentials of 3.0-1.0 V for $Li_4Ti_5O_{12}$ (1) and $Li_{3.624}Ti_{4.944}Ga_{0.2}O_{12}$ (2).

Charge-discharge curves of plain and doped lithium titanate contain well-defined plateaus at potential 1.55 V (Fig. 2a), which reflect the lithium insertion and extraction process by a two-phase

mechanism. The irreversible capacity at the first cycle for all studied samples was 13–16%, but at the second cycle the coulombic efficiency of the cycling for all samples went up to 97%. The discharge capacity of undoped lithium titanate at the current density of 20 mA g^{-1} was about 155 mAh g^{-1}. For the doped sample the discharge capacity was less – about 147 mAh g^{-1}.

Lowering of the discharge capacity of the doped sample is explained by the fact that unlike titanium gallium cannot participate in a redox-process. The theoretical specific capacity of $Li_{3.624}Ti_{4.944}Ga_{0.2}O_{12}$ is about 171 mAh g^{-1} (against 175 mAh g^{-1} for plain lithium titanate). At higher current densities, the discharge capacity of the doped sample exceeds the capacity of $Li_4Ti_5O_{12}$ (Fig. 2b).

Thus, at the current density of 3,200 mA g^{-1} the discharge capacity of $Li_{3.624}Ti_{4.944}Ga_{0.2}O_{12}$ doubles the discharge capacity of $Li_4Ti_5O_{12}$. It should be also noted that after the high-current density cycling and upon return to low current, the discharge capacity of all samples almost coincides with the value registered at the first cycles. It evidences of low cycling degradation of the samples. The calculated values of degradation for all samples did not exceed 0.03 % per cycle.

The enhancing of discharge capacity for doped lithium titanate when cycling in the potential range 1 to 3 V was reported also in [14-18, 22-25].

For example, pristine $Li_4Ti_5O_{12}$ displayed discharge capacity about 33 mAh g^{-1} while for $Li_{3.85}Ni_{0.225}Ti_{4.925}O_{12}$ the capacity was 56 mAh g^{-1} at current density of 800 mA g^{-1} [22]. At current density of 3200 mA g^{-1}, the capacity of the $Li_4Ti_5O_{12}$ was only 30.2 mAh g^{-1}, although, the discharge capacity of the $Li_{3.95}La_{0.05}Ti_5O_{12}$ still remained 54.7 mAh g^{-1} [26].

According to the equation (1), the reversible insertion of one lithium ion corresponds to the specific capacity of about 58 mAh g^{-1}. Thus, it is fair to say that the following brutto-reactions take place at the current density of 20 mA g^{-1} in the range of potentials from 1 to 3 V:

$$Li_4Ti_5O_{12} \pm 2.64e^- \pm 2.64Li^+ \leftrightarrow Li_{6.64}Ti_5O_{12} \quad (2)$$

$$Li_{3.624}Ti_{4.944}Ga_{0.2}O_{12} \pm 2.58e^- \pm 2.58Li^+ \leftrightarrow Li_{6.204}Ti_{4.944}Ga_{0.2}O_{12} \quad (3).$$

According to electrochemical data, after the charge at the current density of 20 mA g^{-1} in the range of potentials from 3 to 1 V undoped lithium titanate has an average composition of $Li_{6.64}Ti_5O_{12}$. It implies that approximately 12% of the material remains uncharged. For $Li_{3.624}Ti_{4.944}Ga_{0.2}O_{12}$ this portion is 14%. Besides, even at a full-charge phase of $Li_7Ti_5O_{12}$ two more titanium ions can be reduced to oxidation state 3+. Thus, a reversible process of lithium insertion-extraction can be continued at potentials more negative than 1V.

When broadening the cycling range up to the potential of 0.01 V, the discharge capacity of plain and doped lithium titanate ($Li_{3.624}Ti_{4.944}Ga_{0.2}O_{12}$) increases, and at the current density of 20 mA g^{-1} it is 258 and 236 mAh g^{-1}, respectively (Fig. 3). It corresponds to approximately 83-85% of the theoretical value of the capacity for both samples in the assumption that the oxidation state of all titanium ions changes to 3+. Thus, it is fair to say that brutto-reactions take place at the current density of 20 mA g^{-1} in the range of potentials from 0.01 to 3 V:

$$Li_4Ti_5O_{12} \pm 4.42e^- + 4.42Li^+ \leftrightarrow Li_{8.42}Ti_5O_{12} \quad (4)$$

$$Li_{3.624}Ti_{4.944}Ga_{0.2}O_{12} \pm 4.1e^- + 4.1Li^+ \leftrightarrow Li_{7.724}Ti_{4.944}Ga_{0.2}O_{12} \quad (5)$$

At low current densities, the cathode branch of the charge-discharge curve can be conditionally divided into four parts (Fig. 3). The first one represents a plateau in the area of potentials of about 1.55

V and corresponds to insertion-extraction of approximately 2.5 lithium ions by a two-phase mechanism with the formation of the materials of brutto-composition of $Li_{6.64}Ti_5O_{12}$ and $Li_{6.124}Ti_{4.944}Ga_{0.2}O_{12}$ for plain and doped titanate, respectively. It is followed by a steep decay down to 0.85 – 0.75 V, conditioned by the fact that shells from $Li_7Ti_5O_{12}$ and $Li_{6.624}Ti_{4.944}Ga_{0.2}O_{12}$ become very thick and high-resistant. The possibility of insertion of 0.5–1 more lithium ions by a two-phase mechanism appears at this potential. On the last inclined section, the potential gradually decreases at further insertion of lithium ions into the compositions of $Li_{8.42}Ti_5O_{12}$ and $Li_{7.764}Ti_{4.944}Ga_{0.2}O_{12}$. Apparently monotone potential shift points out that in this case lithium insertion takes place through the formation of solid solutions. For doped lithium titanate $Li_{3.624}Ti_{4.944}Ga_{0.2}O_{12}$ plateau in the area of potentials of 0.7 V at cathode intercalation of lithium is more expressed than for $Li_4Ti_5O_{12}$. It should be also noted that strong polarization of the undoped sample resulting in the lowered charge and, accordingly, discharge capacities, is observed in case of the increased current density. Only 3 sections are registered on the anode branch of the charge-discharge curve: the first inclined curve in the area of potentials from 0.01 to 0.5 V corresponds to lithium extraction from solid solution with the formation of $Li_7Ti_5O_{12}$ and $Li_{6.624}Ti_{4.944}Ga_{0.2}O_{12}$ for plain and doped lithium titanate, accordingly. Thereafter the potential jumps up to 1.5 V. A plateau that corresponds to lithium extraction by a two-phase mechanism with the formation of $Li_4Ti_5O_{12}$ and $Li_{3.624}Ti_{4.944}Ga_{0.2}O_{12}$, for plain and doped lithium titanate, accordingly, is fixed at this potential.

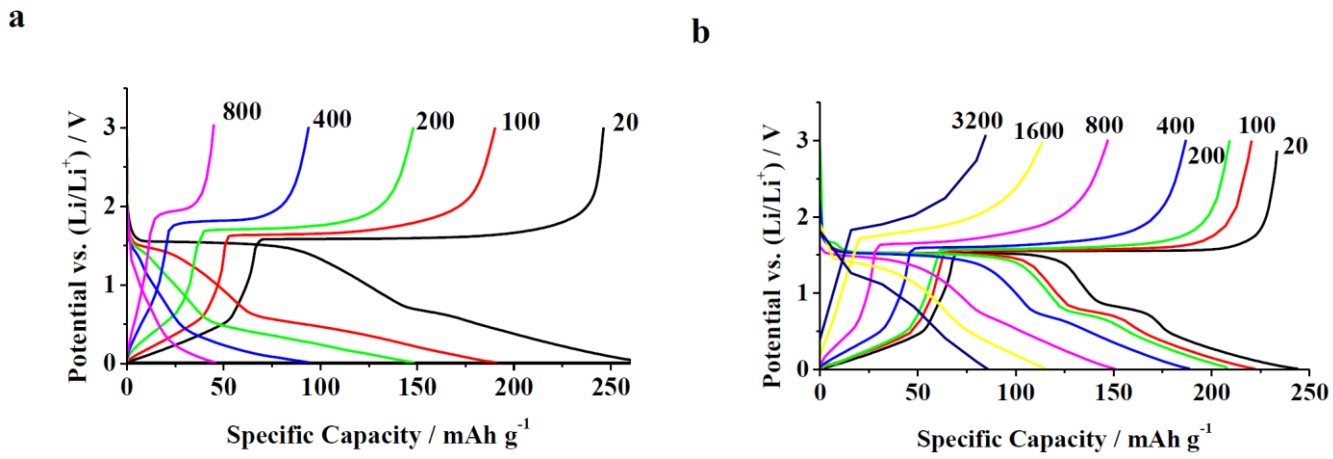

Figure 3. (a) Charge-discharge curves of $Li_4Ti_5O_{12}$ and (b) $Li_{3.624}Ti_{4.944}Ga_{0.2}O_{12}$ in the area of potentials from 0.01 to 3 V at different current densities. Current density in mA g^{-1} is shown in the Figure

Figure 4 shows, the cycling in a wide range of potentials progresses much better for the doped sample. Thus, for $Li_{3.624}Ti_{4.944}Ga_{0.2}O_{12}$ the average capacity loss after 35 cycles did not exceed 0.04 % per cycle. At the same time, it was approximately 5 times higher for the undoped sample. However, during the first cycles at the current density of 20 mA g^{-1} the capacities of the doped and undoped samples become almost equal, and at high current densities the capacity of doped materials becomes significantly higher. At the current densities of 1,600 and 3,200 mA g^{-1} the capacity of the doped sample was 4-5 times higher than for $Li_4Ti_5O_{12}$.

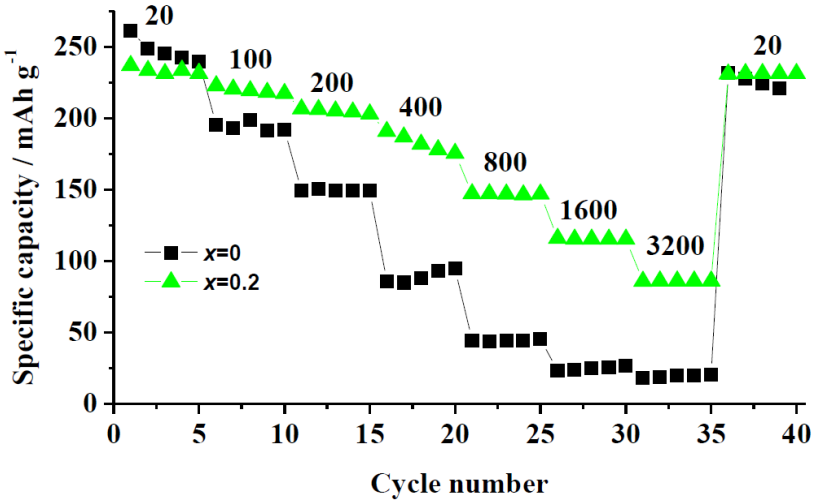

Figure 4. Change in the discharge capacity of $Li_4Ti_5O_{12}$ (1) and $Li_{3.624}Ti_{4.944}Ga_{0.2}O_{12}$ (2) at different current densities. Current density in mA g^{-1} is shown in the Figure.

Table 3 compares the results of the current study with the rate capability taken from the literature for various metallic ion-doped lithium titanate electrodes under lithium insertion up to 0.01 V. It is seen that the discharge capacity for $Li_{3.624}Ti_{4.944}Ga_{0.2}O_{12}$ was 245 mAh g^{-1} at 20 mA g^{-1} and about 85 mAh g^{-1} at 3200 Ma g^{-1}. Close results were obtained for $Li_4Ti_{4.95}Al_{0.05}O_{12}$ [15], however maximal current for this material reached 800 mA g^{-1} only. The discharge capacity for scandium-doped lithium titanate $Li_4Ti_{4.85}Sc_{0.15}O_{12}$ amounted to 225 mAh g^{-1} [28], however it dropped up to 125 mAh g^{-1} at 400 mA g^{-1}. So, the rate capability of $Li_{3.624}Ti_{4.944}Ga_{0.2}O_{12}$ obtained in this study is considered highly comparable or even much better (at the low current density) than the majority of other doped lithium titanate anodes. The only possible exclusion is ruthenium-doped lithium titanate $Li_4Ti_{4.85}Ru_{0.15}O_{12}$, for which the discharge capacity as high as 200 mAh g^{-1} at 17500 mA g^{-1} was reported [31], although this result seems to be rather doubtful.

Table 3. The discharge capacity (mAh g^{-1}) of doped lithium titanate in wide potential range (0.01 – 3 V)

Sample	Current density, mA g^{-1}							
	20	100	200	400	800	1600	3200	Ref
$Li_4Ti_{4.95}Al_{0.05}O_{12}$	225	-	220	200	160	-	-	[15]
$Li_4Ti_{5-x}Bi_xO_{12}$ (x=0.05)	200	-	180	-	150	135	-	
$Li_4Ti_{5-x}Bi_xO_{12}$ (x=0.10)	205	-	185	-	175	155	-	[26]
$Li_4Ti_{5-x}Bi_xO_{12}$ (x=0.15)	205	-	188	-	155	140	-	
$Li_4Ti_{4.8}La_{0.2}O_{12}$	-	-	190	182	175	-	-	[27]
$Li_4Ti_{4.85}Sc_{0.15}O_{12}$	225	175	150	125	-	-	-	[28]
$Li_4Ti_{4.85}Ru_{0.15}O_{12}$	-	-	-	-	250	225	-	[31]
$Li_{3.624}Ti_{4.944}Ga_{0.2}O_{12}$	245	220	200	175	150	120	85	This study

Additional information about reversibility of the lithium insertion-extraction process can be obtained from cyclic voltamograms. Cyclic voltamograms of $Li_4Ti_5O_{12}$ and $Li_{3.624}Ti_{4.944}Ga_{0.2}O_{12}$ at different potential scan rates in the interval of potentials from 1 to 3 V are shown in Fig. 5. The curves of both materials have clear peaks that reflect the lithium insertion and extraction processes, while the forms of the curves of plain and doped lithium titanate differ. Cyclic voltamograms of $Li_{3.624}Ti_{4.944}Ga_{0.2}O_{12}$ have narrower peaks and larger values of specific currents in the peaks of voltamograms. The difference between the potentials of anode and cathode peaks (ΔE) of electrode materials is determined by the reversibility of the lithium insertion-extraction process and specific resistance of phases' materials that are formed during charge and discharge processes. For $Li_{3.624}Ti_{4.944}Ga_{0.2}O_{12}$ ΔE at different potential scan rates, ranged from 85 to 247 mV, while for $Li_4Ti_5O_{12}$ it ranged from 293 to 523 mV. The data from cyclic voltamograms evidence of a greater reversibility of the lithium insertion-extraction process for doped lithium titanate. It should be concluded that increased reversibility is the consequence of increased conductivity of the doped sample against the undoped one.

The dependences of the peak current of voltamograms on the square root of the potential scan rate, shown in the insert in Fig. 5, are linear and go through the origin of coordinates, which evidences of diffusion control of the process of lithium insertion-extraction in plain and doped lithium titanate. Similar CVAs and dependences of the peak current on the square root of scan rate are reported by authors of [11, 14-16, 16, 19, 29]. In particular, ΔE was decreased from 200 to 180 mV upon going from $Li_4Ti_5O_{12}$ to $Li_4Ti_{4.94}Tb_{0.06}O_{12-\delta}$ [29]. With the increase in scan rate, ΔE becomes higher, pointing to increased electrode polarization. Nevertheless, when the scan rate increases to 1.3 mV s^{-1}, the redox peaks of $Li_4Ti_{4.94}Tb_{0.06}O_{12-\delta}$ retain a more stable shape than those of $Li_4Ti_5O_{12}$, implying that $Li_4Ti_{4.94}Tb_{0.06}O_{12-\delta}$ has weaker polarization [29].

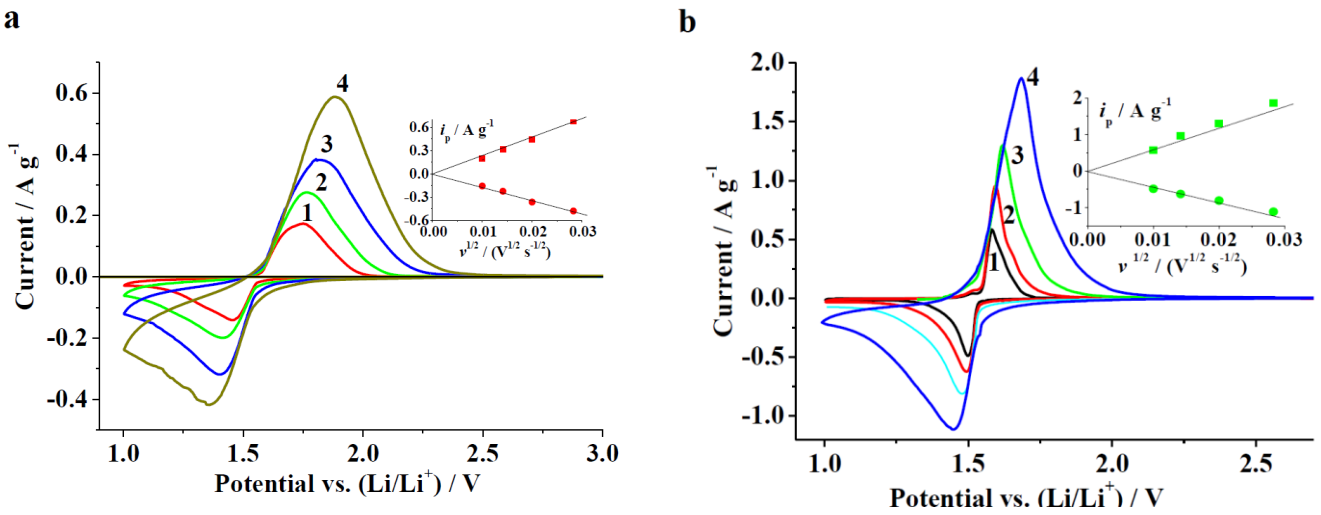

Figure 5. Cyclic voltamograms of the samples of $Li_4Ti_5O_{12}$ (a) and $Li_{3.624}Ti_{4.944}Ga_{0.2}O_{12}$ (b) in the range of potentials from 1 to 3 V. Potential scan rates (μV s^{-1}): 1 – 100, 2 – 200, 3 – 400, 4 – 800.

When the potential scan range increases, the form of cyclic voltamograms significantly changes (Fig. 6). Two cathode peaks are registered on the cathode part of cyclic voltamograms: in the area of potentials of 1.5 – 1.55 V (marked as I in the Figure, hereinafter the area of the first cathode peak) and in the area of potentials of 0.6 – 0.7 V (marked as II in the Figure, hereinafter the area of the second cathode peak). Both cathode peaks reflect lithium insertion by a two-phase mechanism. Subsequent lithium insertion with the formation of a solid solution is described by a wave in the area of potentials of 0.6 – 0.01 V. Lithium extraction in the area of potentials from 0.01 to 0.7 V is described by a faint peak, which corresponds to a solid solution. Lithium extraction by a two-phase mechanism is described by clear peaks in the area of potentials from 1.5 to 3 V. The cathode peak at potentials of 0.6 – 0.7 V can be also attributed to the process of the electrolyte reduction with the formation of a solid electrolyte interface (SEI). Indeed, the current in the cathode peak at potentials of 0.6 – 0.7 at the first cycle is higher than that at the second cycle and, consequently, some charge is spent on the formation of SEI. However, this peak is registered not only at the first, but at all subsequent cycles, and, consequently, the cathode peak of the area of potentials of 0.6 – 0.7 V should be attributed to lithium insertion by a two-phase mechanism. The authors of [15, 26–28, 30] have registered the appearance of the second peak at 0.6–0.7 V as well. Unfortunately, the authors of [15, 26, 27] don't explain an origin of the peak. The authors of [28] ascribe this peak to SEI formation. According to authors of [30] the second peak at 0.6 V is connected with reduction of Ti^{4+} to Ti^{3+}, which suggested a multistep restore of Ti^{4+} during the discharge period. It can be found a broad peak with envelope feature at lower potentials, indicating a formation of an amorphous phase during discharge to 0 V.

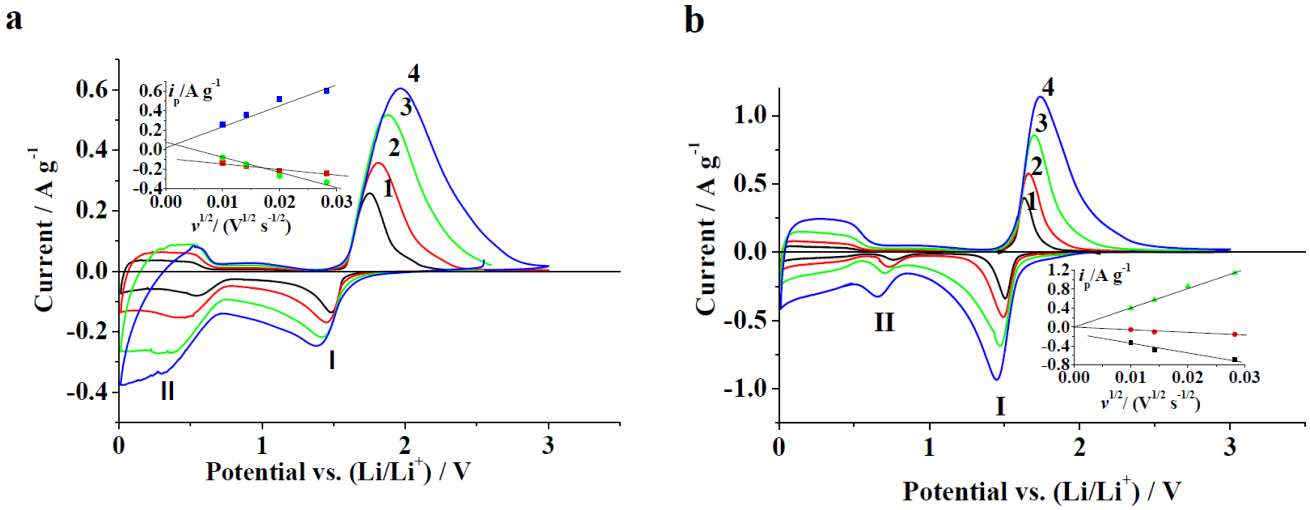

Figure 6. Cyclic voltamograms of $Li_4Ti_5O_{12}$ (a) and $Li_{3.624}Ti_{4.944}Ga_{0.2}O_{12}$ (b) in the range of potentials 0.01 – 3 V. Potential scan rates (mV s^{-1}):1 – 0.1, 2 – 0.2, 3 – 0.4, 4 – 0.8.

The comparison of cyclic voltamograms of doped and undoped lithium titanate shows that for the doped sample the second cathode peak (0.6 – 0.7 V), corresponding to a two-phase lithium insertion mechanism for the doped sample, is registered at more positive potentials, which evidences of the higher conductivity of the doped sample. Besides, ΔE for $Li_{3.624}Ti_{4.944}Ga_{0.2}O_{12}$ turns out to be

half as many as ΔE for $Li_4Ti_5O_{12}$, which also evidences of the higher reversibility of the lithium insertion-extraction process for the doped sample.

The calculated data (Table 4) obtained from cyclic voltamograms are in good agreement with the data from galvanostatic measurements, namely, at a small potential scan rate (0.1 mV s^{-1}) the discharge capacity of plain lithium titanate slightly exceeds the discharge capacity of doped lithium titanate. Simultaneously, the situation is reverse when the potential scan rate increases. Thus, when v=0.4 mV s^{-1} the discharge capacity of $Li_{3.624}Ti_{4.944}Ga_{0.2}O_{12}$ exceeds the discharge capacity of $Li_4Ti_5O_{12}$, and when v=0.8 mV s^{-1} the discharge capacity of $Li_{3.624}Ti_{4.944}Ga_{0.2}O_{12}$ is 1.5 times higher than that of $Li_4Ti_5O_{12}$.

One of the explanations of higher values of the discharge capacity may be an increased lithium effective diffusion coefficient (D_{eff}) at gallium doping of lithium titanate. To confirm this assumption, D_{eff} for both materials were calculated based on the data from cyclic voltamograms during the cycling at different ranges of potentials.

The Randles–Ševcik equation was used for calculation:

$$D^{1/2} = i_p v^{-½} \; 2.69\ 10^5 S c$$

Where i_p is a peak current, v is the potential scan rate (V s^{-1}), S is the true area of the surface (cm^2), and c is the concentration of lithium ions (mole cm^{-3}).

Table 4. Calculated data for $Li_4Ti_5O_{12}$ and $Li_{3.624}Ti_{4.944}Ga_{0.2}O_{12}$ obtained from cyclic voltamograms

Potential scan rate, mV s^{-1}	Capacity in cathode half-cycle (Q_k), mAh g^{-1}		Capacity in anode half-cycle (Q_a), mAh g^{-1}		ΔE, mV	
	$Li_4Ti_5O_{12}$	$Li_{3.624}Ti_{4.944}Ga_{0.2}O_{12}$	$Li_4Ti_5O_{12}$	$Li_{3.624}Ti_{4.944}Ga_{0.2}O_{12}$	$Li_4Ti_5O_{12}$	$Li_{3.624}Ti_{4.944}Ga_{0.2}O_{12}$
in the range of potentials 1 – 3 V						
0.1	118	142	122	125	293	85
0.2	104	130	110	122	357	100
0.4	99	117	98	116	428	147
0.8	79	108	78	107	523	247
in the range of potentials 0.01 – 3 V						
0.1	256	240	248	232	0.274	0.126
0.2	236	231	235	230	0.367	0.172
0.4	199	222	198	221	0.485	0.225
0.8	139	204	138	203	0.588	0.292

At the cycling in a narrow range of potentials, the concentration of lithium ions for $Li_4Ti_5O_{12}$ and $Li_{3.624}Ti_{4.944}Ga_{0.2}O_{12}$ amounted to 0.022 and 0.0196 mole cm^{-3}, respectively. The effective diffusion coefficient at the insertion of lithium ions into $Li_4Ti_5O_{12}$ and $Li_{3.624}Ti_{4.944}Ga_{0.2}O_{12}$ was $7.35*10^{-10}$ and $1.65*10^{-9}$ cm^2 s^{-1}, accordingly. At the extraction of lithium, the effective diffusion coefficient of lithium ions from $Li_4Ti_5O_{12}$ and $Li_{3.624}Ti_{4.944}Ga_{0.2}O_{12}$ amounted to $1.48*10^{-9}$ and $7.0*10^{-9}$ cm^2 s^{-1}, accordingly. According to [14] the calculated lithium diffusion coefficient D_{Li+} in $Li_4Ti_{4.995}Ta_{0.005}O_{12}$ is $3.01*10^{-10}$ cm^2 s^{-1}, while that of the pristine $Li_4Ti_5O_{12}$ is only $7.55*10^{-12}$ cm^2 s^{-1}.

It can be found that the diffusivity with $Li_4Ti_{4.95}Al_{0.05}O_{12}$ was $6.49*10^{-10}$ cm^2 s^{-1}, which was slightly larger than that with the $Li_4Ti_5O_{12}$ ($2.71*10^{-10}$ cm^2 s^{-1}) [15]. Table 5 demonstrates the excellent coincidence of the diffusion coefficient obtained in the present study with the literature data.

Table 5. Calculated diffusion coefficients Li^+ ions at 25 °C for the samples

Sample	$D_{eff}^{reduction}$, cm^2 s^{-1}	$D_{eff}^{oxidation}$, cm^2 s^{-1}	Ref.
$Li_{3.9}Ti_{4.8}Cr_{0.03}O_{12}$	$6.4*10^{-9}$	$3.1*10^{-9}$	[11]
$Li_4Ti_{4.995}Ta_{0.005}O_{12}$	$3.01*10^{-10}$	-	[14]
$Li_4Ti_{4.95}Al_{0.05}O_{12}$	-	$6.49*10^{-10}$	[15]
$Li_4Ti_{4.94}Tb_{0.06}O_{12-\delta}$	-	$7.86*10^{-9}$	[29]
$Li_{3.624}Ti_{4.944}Ga_{0.2}O_{12}$	$1.65*10^{-9}$	$7.0*10^{-9}$	This study

At the cycling in a wide range of potentials, cyclic voltamograms register two cathode maximums and one anode maximum, which can allow calculating diffusion coefficients at the insertion of lithium at different potentials. Meanwhile, the dependence of cathode currents in the peaks on the square root of the potential scan rate does not go through the origin of coordinates, which evidences of activation and diffusion (mixed) control of the lithium insertion-extraction process. The dependence of anode peaks goes through the origin of coordinates, which evidences of diffusion control of the lithium insertion-extraction process. Lithium ions concentration at their extraction amounted to 0.03 mole cm^{-3}. The value of lithium effective diffusion coefficient at lithium extraction is 2.9 and $3.1*10^{-9}$ for $Li_4Ti_5O_{12}$ and $Li_{3.624}Ti_{4.944}Ga_{0.2}O_{12}$, accordingly. So, it can be inferred that gallium doping of lithium titanate results in the increased lithium effective diffusion coefficient.

The cathode peak in the area of potentials 0.6-0.7 V, as is described above, is conditioned by difficulties related to the passage of lithium through the forming shell of $Li_{6.624}Ti_{4.944}Ga_{0.2}O_{12}$.

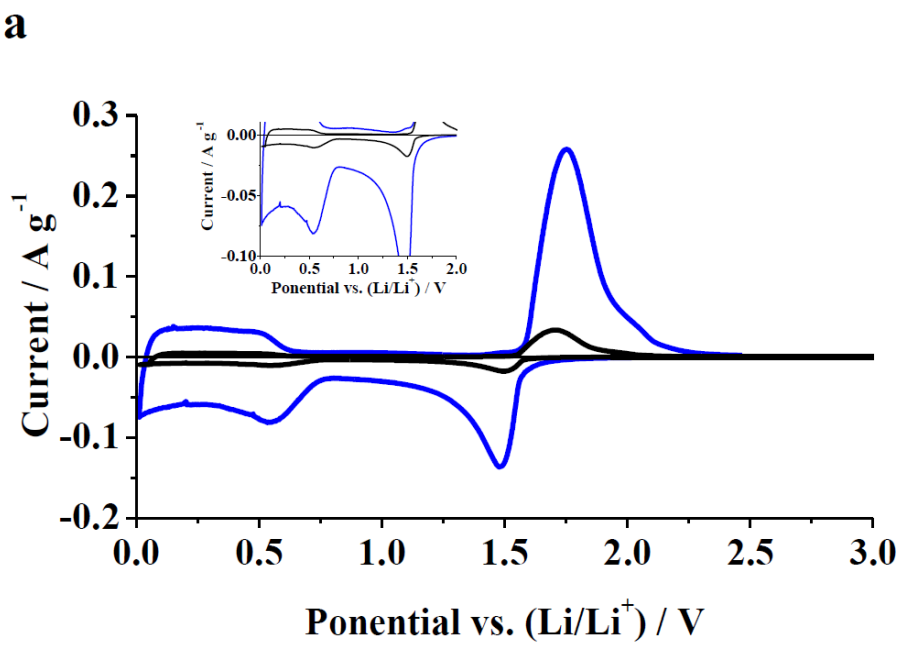

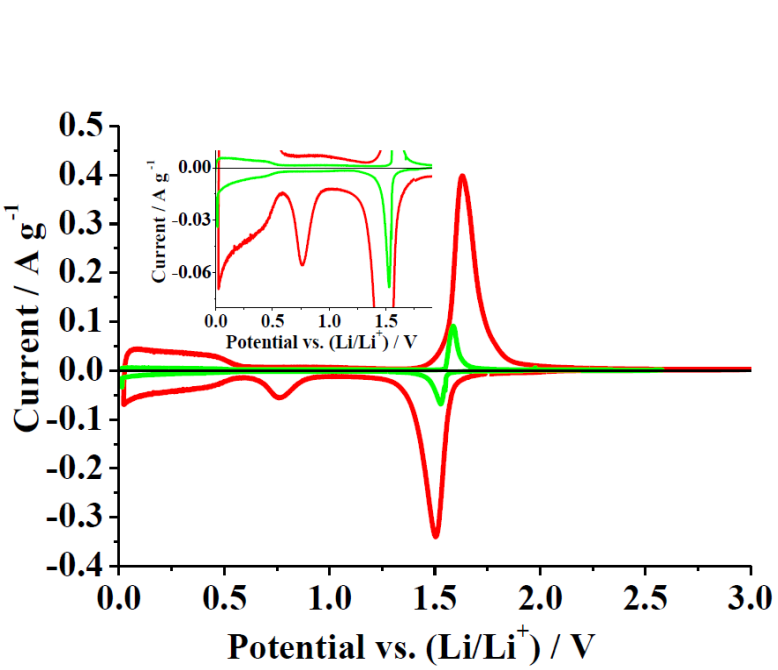

Figure 7. Cyclic voltamograms of $Li_4Ti_5O_{12}$ (a) and $Li_{3.624}Ti_{4.944}Ga_{0.2}O_{12}$ (b) in the range of potentials 0.01 – 3 V. Potential scan rates (mV s^{-1}):1 – 0.01, 2 – 0.1.

Under that logic, decrease in the potential scan rate at registration of cyclic voltamograms or the current density at galvanostatic cycling must result in the reduction (or complete disappearance) of the lithium insertion process by a two-phase mechanism in the area of potentials of 0.6–0.7 V. To confirm this hypothesis, cyclic voltamograms were registered at a very low potential scan rate – 0.01 mV/s and the obtained data were compared with the data at higher potential scan rates (Fig 7).

Really, for $Li_{3.624}Ti_{4.944}Ga_{0.2}O_{12}$ at a scan rate of 0.01 mV s^{-1} the peak at the potential about 0.7 V completely disappears. It means that the process of insertion of lithium with the two-phase mechanism proceeds only in the area of potentials from 3 to 1 V. Discharge capacity was about 170 and 280 mAh g^{-1} at end potential of 1.0 and 0.01 V, respectively. At the same time, for $Li_4Ti_5O_{12}$ even at so small scan rate the cathodic peak at the potential of 0.6 V has been registered. Cathodic capacity at this scan rate was about 150 and 260 mAh g^{-1} at the end potential of 1.0 and 0.01 V, respectively. Thus, the result of the cyclic voltammograms received at a low scan rate also confirms increase in conductivity of gallium-doped lithium titanate.

4. CONCLUSION

Gallium-doped lithium titanate was synthesized using the citrate method. According to the data obtained as a result of updating the structure using the Rietveld method of the sample of $Li_{4+z}Ti_{5-z}Ga_zO_{12}$ composition at z=0.1, gallium ions occupy both, positions of lithium (8a), and positions of titanium (16d). Moreover, there are about 2.5 times less of gallium ions in octahedral sites than in tetrahedral ones. In accordance with these results, the formula of gallium-doped lithium titanate should be as follows: $Li_{4+x-3y}Ti_{5-x}Ga_{x+y}O_{12}$ (x+y=0.1-0.2; y/x=2.56). Thus, when the doping degree is

x+y=0.2, the formula is as follows: $Li_{3.624}Ti_{4.944}Ga_{0.2}O_{12}$. Electrochemical measurements have proved ability of gallium-doped lithium titanate to operate in wide potential range without degradation. In this case the discharge capacity of $Li_{3.624}Ti_{4.944}Ga_{0.2}O_{12}$ was about 250 and 85 mAh g^{-1} at current density of 20 and 3200 mA g^{-1}, respectively. At the same time undoped lithium titanate cannot operate at current densities higher than 800 mA g^{-1} in wide potential range.

ACKNOWLEDGMENTS
The research was financially supported by the Russian Foundation for Basic Research (Project No. 14-29-04068 ofi_m).

References

1. C. Julien, A. Mauger, A. Vijh, K. Zaghib, *Lithium Batteries: Science and Technology*, N.-Y.: Springer, 2015. 619 p.
2. A. Yaroslavtsev, T. Kulova, A. Skundin, *Russ. Chem. rev*., 84 (2015) 826.
3. S. Schamer, W. Weppner, P. Schmid-Beurmann, *J. Electrochem. Society*, 146 (1999) 857.
4. B. Zhao, R. Ran, M. Liu, Z. Shao, *Materials Science and Engineering*, R98 (2015) 1.
5. J. Shu., *J. Solid State Electrochemistry*, 13 (2009) 1535.
6. X. Yao, S. Xie, H. Nian, *Journal of Alloys and Compounds*, 465 (2008) 375.
7. Z. Yang, D. Choi, S. Kerisit, K. Rosso, D. Wang, J. Zhang, G. Graff, J. Liu, *J. Power Sources*, 192 (2009) 588.
8. T. Yi, L. Jiang, J. Shu, C. Yue, R. Zhu, H. Qiao, *J. Phys.Chem. Solids*, 71 (2010) 1236.
9. C. Chen, J. Vaughey, A. Jansen, D. Dees, A. Kahaian, T. Goacher, M. Thackeray, *J. Electrochem. Soc.*, 148 (2001) A102.
10. M. Wilkening, R. Amade, W. Iwaniak, P. Heitjans, *Phys. Chem. Chem. Phys*., 9 (2007) 1239.
11. F. Wu, X. Li, Z. Wang, H. Guo, *Ceramics International*, 40 Part B (2014) 13195.
12. P. Du, L. Tang, X. Zhao, W. Weng, G. Han, *Surface and Coatings Technology*, 198 (2005) 395.
13. X. Wu, Zh. Wen, X. Wang, X. Xu, J. Lin, Sh. Song, *Fusion Engineering and Design*, 85 (2010) 1442.
14. M. Guo, S. Wang, L. Ding, C. Huang, H. Wang, *J. Power Sources*, 283 (2015) 372.
15. J. Lin, C. Hsu, H. Ho, Sh. Wu, *Electrochim. Acta*, 87 (2013) 126.
16. Y. Zhang, C. Zhang, Y. Lin, D. Xiong, D. Wang, X. Wu, *J. Power Sources*, 250 (2014) 50.
17. C. Lin, B. Ding, Y. Xin, F. Cheng, M. Lai, L. Lu, H. Zhou, *J. Power Sources*, 248 (2014) 1034.
18. G. Hu, X. Zhang, Z. Peng, *Transactions of Nonferrous Metals Society of China*, 21 (2011) 2248.
19. M. Guo, H. Chen, S. Wang, Sh. Dai, L. Ding, H. Wang, *J. Alloys and Compounds*, 687 (2016) 746.
20. T. Kulova, Yu. Kreshchenova, A. Kuz'mina, A. Skundin, I. Stenina, A. Yaroslavtsev, *Mendeleev Communications*, 26 (2016) 238.
21. S. Huang, Z. Wen, X. Zhu, Z. Lin, *J. Power Sources*, 165 (2007) 408.
22. C. Lin, M. Lai, L. Lu, H. Zhou, Y. Xin, *J. Power Sources*, 244 (2013) 272.
23. Z. Zhang, L. Cao, J. Huang, S. Zhou, Y. Huang, Y. Cai, *Ceramics International*, 39 (2013) 6139.
24. Q. Zhang, X. Li, *Int. J. Electrochem. Sci.*, 8 (2013) 7816.
25. D. Wang, C. Zhang, Y. Zhang, J. Wang, D. He, *Ceramics International*, 39 (2013) 5145.
26. T. Subburaj, K. Prasanna, K. Kim, P. Ilango, Y. Jo, C. Lee, *J. Power Sources*, 280 (2015) 23.
27. T. Yi, Y. Xie, Q.Wu, H. Liu, L. Jiang, M. Ye, R. Zhu, *J. Power Sources*, 214 (2012) 220.
28. S. Yang, J.Yuan, Y. Zhu, T.Yi, Y. Xie, *Ceramics International*, 41 (2015) 7073.
29. P. Zhang, Y. Huang, W. Jia, Y. Cai, X. Wang, Y. Guo, D. Jia, Z. Sun, Z. Guo, *Electrochim. Acta, 210 (2016) 935.*

30. T. Yi, Z.Fang, L. Deng, L.Wang, Y. Xie, Y. Zhu, J. Yao, C. Dai, *Ceramics International*, 41 (2015) 2336.
31. W. Wang, H. Wang, S. Wang, Y. Hu, Q. Tian, S. Jiao, *J. Power Sources*, 228 (2013) 244.

© 2017 The Authors. Published by ESG (www.electrochemsci.org). This article is an open access article distributed under the terms and conditions of the Creative Commons Attribution license (http://creativecommons.org/licenses/by/4.0/).